Jpn J Radiol
DOI 10.1007/s11604-012-0147-7

ORIGINAL ARTICLE

Diffusional kurtosis imaging of normal-appearing white matter in multiple sclerosis: preliminary clinical experience

Mariko Yoshida · Masaaki Hori · Kazumasa Yokoyama · Issa Fukunaga · Michimasa Suzuki · Koji Kamagata · Keigo Shimoji · Atsushi Nakanishi · Nobutaka Hattori · Yoshitaka Masutani · Shigeki Aoki

Received: 25 July 2012 / Accepted: 25 September 2012

Abstract
Purpose We evaluated diffusional changes in normal-appearing white matter (NAWM) regions remote from multiple sclerosis (MS) plaques by using diffusional kurtosis imaging (DKI) to investigate the non-Gaussian behavior of water diffusion.
Materials and methods Participants were 11 MS patients and 6 age-matched healthy volunteers. DKI was performed on a 3-T MR imager. Fractional anisotropy (FA), apparent diffusion coefficient (ADC), and diffusional kurtosis (DK) maps were computed. Regions of interest (ROIs) were compared in 24 cerebral regions, including the frontal, parietal, and temporal lobe white matter (WM) in controls and NAWM in MS patients.
Results The mean FA of all ROIs was 0.468 ± 0.014 (SD) (controls) or 0.431 ± 0.029 (MS group) ($P = 0.016$). Mean ADC was $0.785 \pm 0.034 \times 10^{-3}$ mm^2/s (controls) or $0.805 \pm 0.041 \times 10^{-3}$ mm^2/s (MS group). The mean DK of all ROIs was 0.878 ± 0.020 (controls) or 0.823 ± 0.032 (MS group) ($P = 0.002$). Analysis of individual ROIs revealed significant differences in DK in 3 ROIs between normal WM and NAWM, but significant differences in ADC and FA in only one ROI each.
Conclusion DKI may be a new sensitive indicator for detecting tissue damage in MS patients in addition to conventional diffusional evaluations, for example diffusion tensor imaging.

Keywords Diffusional kurtosis · MRI · DKI · Non-Gaussian · Multiple sclerosis · Normal-appearing white matter

Introduction

In multiple sclerosis (MS), diffusion analysis of water molecules using magnetic resonance imaging (MRI) is a quantitative technique for revealing more specific microstructural changes than conventional MRI. It enables the apparent diffusion coefficient (ADC) in the tissues to be calculated. The ADC reflects the microscopic Brownian motion of water molecules [1]. It has been reported to be very sensitive to the occult tissue damage of MS, and has revealed abnormalities of diffusion MRI metrics in the normal-appearing white matter (NAWM) outside plaques of MS patients; in MS the ADC in the NAWM was elevated [2–4].

Diffusion tensor imaging (DTI) provides a mathematical description of the magnitude and directional dependency (anisotropy) of the movement of water molecules in three-dimensional space [5]. It furnishes, separately, indices of fractional anisotropy (FA) and ADC in three-dimensions [1]. Recent studies have shown that DTI can quantify the extent and pathological severity of the structural changes occurring within MS plaques and in the NAWM [6–8].

M. Yoshida (✉) · M. Hori · M. Suzuki · K. Kamagata · K. Shimoji · A. Nakanishi · S. Aoki
Department of Radiology, Juntendo University School of Medicine, 2-1-1 Hongo, Bunkyo-ku, Tokyo 113-8431, Japan
e-mail: mrk.ysd@gmail.com; mryoshi@juntendo.ac.jp

K. Yokoyama · N. Hattori
Department of Neurology, Juntendo University School of Medicine, Tokyo, Japan

I. Fukunaga
Graduate School of Health Promotion Science, Tokyo Metropolitan University, Tokyo, Japan

Y. Masutani
Division of Radiology and Biomedical Engineering, Graduate School of Medicine, The University of Tokyo, Tokyo, Japan

Published online: 23 October 2012

Moreover, previous investigators have noted reduced FA and elevated ADCs in both MS plaques and NAWM, with higher ADCs in the plaques than in the NAWM [4, 9–11].

Diffusional kurtosis imaging (DKI) is an emerging MRI technique that provides information about non-Gaussian water diffusion in tissues [12, 13]. DKI can furnish diffusional non-Gaussianity, called diffusional kurtosis (DK), and the standard DTI metrics, for example FA and ADC. An advantage of DK over FA is that, because DK does not rely on spatially oriented tissue structures, it can be used to evaluate both gray and white matter (WM). Moreover, unlike DTI, DKI is not affected by crossing fiber tracts [14]. We evaluated diffusional changes in the NAWM regions remote from MS plaques by using DKI in a clinically appropriate setting.

Methods

Subjects

The subjects were 11 MS patients (4 men and 7 women; mean age, 38.4 ± 8.5 SD years) and 6 healthy volunteers (3 men and 3 women, mean age 35.3 ± 5.9 years) with no history of neurological disease. Informed consent was obtained from all patients and volunteers. The local ethics committee approved this study.

All of the MS patients had relapsing–remitting MS, defined according to standard criteria [15–17]; the median Expanded Disability Status Scale [18] at study entry was 1.77 (range 0–6.0), and the mean disease duration was 9.76 ± 7.71 years.

Imaging procedure

Our data for diffusion metrics were acquired on a 3-T magnetic resonance scanner (Achieva; Philips Medical Systems, Best, The Netherlands) with an 8-channel-array SENSE head coil. After conventional imaging sequences had been taken, including T2 and T1-weighted images and fluid-attenuated inversion recovery (FLAIR) images, DKI was acquired by use of a single-shot, spin–echo echo planar imaging (EPI) sequence following repetition time/echo time, 3000/80 ms; number of signals acquired: one; section thickness: 5 mm, 20 slices; field of view: 256 × 256 mm; matrix: 128 × 128; imaging time: approximately 13 min; and six diffusion weighting (b) values (0, 500, 1000, 1500, 2000, and 2500 s/mm^2), with diffusion encoding in 32 directions for every b value. Gradient length (δ) was kept at 27.7 ms, and the time between the two leading edges of the diffusion gradient (Δ) was kept at 39.2 ms. A b value of 2500 s/mm^2 was used as a reference value for consistency with recent reports [12, 13].

Diffusion metrics

B0 distortion correction was applied to all diffusion data on the magnetic resonance imager. DKI data were transferred to an offline workstation. Diffusion metric maps were calculated by using the free software dTV II FZR (Image Computing and Analysis Laboratory, Department of Radiology, The University of Tokyo Hospital, Japan). FA and ADC maps and color maps with 3-dimensional (x, y, z) information using a conventional mono-exponential model were obtained, as were DK maps.

Regions of interest (ROIs) were determined in NAWM in the MS group and normal WM in the control group, and the values of FA, ADC, and DK (also known as mean DK or mean kurtosis, defined as the average of the kurtosis over all possible diffusion directions, were compared in these regions.

The DKI pulse sequence and processing algorithm have been described previously [12, 13]. Briefly, this technique uses a diffusion-sensitizing pulse sequence and the signal intensity data are fitted to the functional form [12, 19]:

$$S = S_0 \exp\left(-bD_{\text{app}} + \frac{1}{6}b^2 D_{\text{app}}^2 K_{\text{app}}\right) \quad \text{(A)}$$

where S_0 is the signal intensity for $b = 0$, D_{app} is the ADC, and K_{app} is the apparent diffusional kurtosis (ADK). The Stejskal–Tanner sequence [20] was defined such that the b-value is given by $b = (\gamma\delta g)^2(\Delta - \delta/3)$, where γ is the nuclear spin gyromagnetic ratio, g is the diffusion time, and Δ and δ were as given above (in the section "Imaging procedure"). Parametric maps of the ADK and ADC were created by fitting the image signal intensities on a voxel-by-voxel basis to Eq. (A), as described elsewhere [12, 19]. The conventional DTI data were calculated by using information at the b value, 1000.

Image analysis

First, we checked the MS patients' plaques on the FLAIR images and T2-weighted echo-planar images. The 24 ROIs were placed on NAWM in the MS group by using the T2-weighted echo-planar images or color maps. Particular care was taken to avoid contamination by MS plaques close to the NAWM (Fig. 1). None of the ROIs were in the MS plaques and peripheral plaques. ROIs were also drawn in matching regions in the WM of the age-matched controls. FA, ADC, and DKI were calculated by using the free software dTV II FZR. All of the ROIs were fixed at the same size, 19 voxels (total: 152 mm^3); each voxel was an interpolated 2-mm isotropic voxel with cubic shape. The size of ROIs selected was as large as possible in order not to deviate from all WM regions.

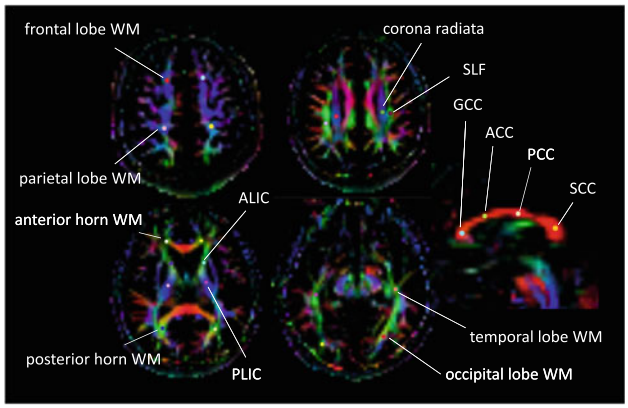

Fig. 1 Examples of the drawing of 24 regions of interest. Particular care was taken to avoid contamination by plaques close to the normal-appearing white matter. *WM* white matter, *ALIC* anterior limb of internal capsule, *PLIC* posterior limb of internal capsule, *SLF* superior longitudinal fasciculus, *GCC* genu of corpus callosum, *ACC* anterior corpus callosum, *PCC* posterior corpus callosum, *SCC* splenium of corpus callosum

The 24 ROIs consisted of 10 bilateral areas—frontal lobe WM, parietal lobe WM, superior longitudinal fasciculus (SLF), corona radiata, peripheral WM of anterior horn of lateral ventricle and posterior horn of lateral ventricle, anterior limb of internal capsule (ALIC), posterior limb of internal capsule (PLIC), occipital lobe WM, temporal lobe WM, and the 4 ROIs on the corpus callosum that were not bilateral (the genu (GCC), the anterior (ACC), the posterior (PCC), and the splenium (SCC)).

Statistical analysis

The Mann–Whitney test was performed to assess differences in the averaged values of FA, ADC, and DK between the 11 patients and 6 healthy control subjects. IBM SPSS Statistics software (version 19.0, SPSS, Chicago, IL, USA) was used. $P < 0.05$ was considered to indicate a statistically significant difference.

For comparison of the 24 individual ROIs in the normal WM and NAWM, Mann–Whitney *U* tests with Bonferroni correction were performed to compare the averaged FA, ADC, and DK values between MS patients and normal controls. $P < 0.05$ (with Bonferroni correction, $P < 0.002$) was considered to indicate a statistically significant difference.

Results

Analysis of mean values of FA, ADC, and DK in all ROIs

The mean values and standard deviations (SD) are shown in Table 1.

Table 1 Averages and standard deviations (SD) of fractional anisotropy (FA), apparent diffusion coefficient (ADC), and diffusional kurtosis (DK) values for all the ROIs

	FA	ADC ($\times 10^{-3}$ mm^2/S)	DK
Controls	0.468 ± 0.014	0.785 ± 0.034	0.878 ± 0.020
MS patients	0.431 ± 0.029	0.805 ± 0.041	0.823 ± 0.032

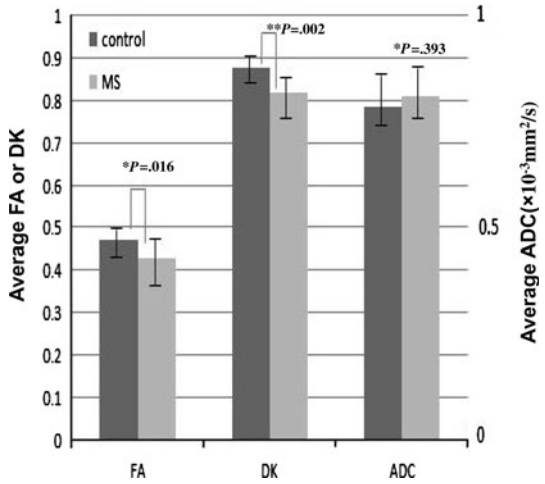

Fig. 2 Averages of fractional anisotropy (FA), diffusional kurtosis (DK), and apparent diffusion coefficient (ADC) in control and multiple sclerosis (MS) groups. Significant differences in FA and DK were observed between the control and MS groups

The mean FA for all ROIs was 0.468 ± 0.014 SD in the control group and 0.431 ± 0.029 in the MS group. The mean ADC was 0.785 ± 0.034 × 10^{-3} mm^2/s in the control group and 0.805 ± 0.041 × 10^{-3} mm^2/s in the MS group. The mean DK of all ROIs was 0.878 ± 0.020 in the control group and 0.823 ± 0.032 in the MS group.

Significant differences in mean FA ($P = 0.016$) and, particularly, in DK ($P = 0.002$), were observed between normal WM and NAWM. ADC values were non-significantly higher in the MS group than in the control group ($P = 0.393$). These analyses are summarized in Fig. 2.

Analysis of individual ROIs in normal WM and NAWM

Mann–Whitney *U* tests revealed marked differences ($P < 0.05$) in FA in 4 ROIs (right parietal lobe WM, left temporal lobe WM, PCC, and SCC) between the control and MS groups. Marked differences ($P < 0.05$) in ADC were observed in 5 ROIs (right SLF, temporal lobe WM bilaterally, PCC, and SCC) between the control and MS groups. Marked differences ($P < 0.05$) in DK were observed in 6 ROIs (right SLF, temporal lobe WM

bilaterally, left frontal lobe WM, PCC, and SCC) between the control and MS groups.

Bonferroni correction revealed significant differences ($P < 0.002$) in FA in one ROI (right parietal lobe WM) between normal WM and NAWM. Significant differences in ADC were observed in one ROI (left temporal lobe WM) between the control and MS groups. Significant differences in DK were observed in 3 ROIs (right SLF, left temporal lobe WM, and SCC) between the control and MS groups.

Discussion

MS is an autoimmune-mediated disease of the central nervous system; its lesions are characterized by inflammation, edema, demyelination, remyelination, axonal damage, gliosis, or a combination of these features [21–25]. Recently these findings have been known as neurodegenerative phenomena [24]. Neuronal/axonal damage and gray matter and WM atrophy are important in disease progression [24, 25].

Conventional MRI is the primary imaging modality that supports clinical diagnosis of MS [26, 27]; quantitative analysis, especially using histograms, have been reported [28–30]. However, it is limited to low pathological specificity and quantitative evaluation of the WM outside visible lesions on T2-weighted images or FLAIR. Therefore, it cannot be used to evaluate diffuse damage in the NAWM and the association of this damage with clinical status.

DTI is a quantitative technique that can be used to overcome these limitations. Recent studies have found that DTI can reveal subtle damage in the NAWM of MS patients [31, 32]. DTI studies have shown that MS plaques and NAWM have significantly higher average ADCs and significantly lower average FAs than healthy WM, and that NAWM injury becomes more pronounced with increasing disease duration and clinical disability [8, 31, 32].

However, DTI presupposes a Gaussian approximation of the diffusion displacement in an unrestricted environment whereas diffusion is, in reality, restricted by barriers of cell membranes, axon sheaths, and water compartments, etc. DTI cannot be used to measure non-Gaussian diffusion; moreover, it may not be used to predict accurate values at dense intersections of fiber tracts [33]. In contrast, DKI can be used to quantify non-Gaussian diffusion and is a more sensitive indicator of diffusional heterogeneity [12, 19, 34]. Diffusional non-Gaussianity may arise from diffusion barriers, for example cell membranes, axon sheaths, myelin layers and organelles, and water compartments. DKI can be regarded as an indicator of microstructural complexity and can be used to investigate abnormalities in tissues with isotropic structure, i.e. gray matter and WM [12].

It has already been shown that the DKI method can be used to detect changes in tissue microstructure between healthy subjects and patients with white matter lesions [35], during normal human aging [36], during rodent brain maturation [37], in staging of cerebral gliomas [38], after mild brain injury [39, 40], in attention-deficit hyperactivity disorder [41], in cerebral infarction [42], and in lung/small airway disease [43].

Histological studies in MS have revealed pathological damage in WM areas that have appeared normal on conventional MRI. This damage consists of astrogliosis, microglial activation, vascular hyalinization, blood–brain-barrier breakdown, reduced myelin density, and axonal loss [44].

Our results showed that DKI could detect abnormalities in NAWM that could not be imaged by conventional MRI. Differences in DK between NAWM and normal WM were more pronounced than those in FA or ADC. Our results suggest that DKI is sensitive to microstructural changes associated with the above pathology by quantifying diffusional non-Gaussianity. DK is believed to be sensitive to slow diffusional movement in a restricted environment, which may be mainly determined by microstructure. As a consequence of our results, DKI can provide the additional information and be a more precise biomarker of tissue damage in NAWM in MS patients compared with DTI (FA and ADC). More sensitive evaluation of NAWM could enable prediction of clinical status and be used as a tool for monitoring the responses of MS patients to medication.

Limitations of our study include the small number of patients and a possible need to further optimize the procedure used for data acquisition with DKI. Normalization of DK data would be needed if this technique were to be compared with others, for example DTI and q-space imaging. Because our study was an ROI study, it could be regarded as subjective and assessment of a small area of WM. More types of statistical analysis (e.g., of the automatic ROI setting or the use of histogram analysis [28, 29]) are being considered, and we need to attempt tract-specific analysis of the WM in MS. This study focused on comparison of normal WM and NAWM. It is necessary for us to assess lesions, including some types of plaques, in MS to determine their elaborate pathological changes. Moreover, studies of the correlation between clinical findings (e.g., cognitive function or clinical stages) and imaging data will be needed. Another limitation is that we used only mean DK. Recently studies of directional DK, i.e. axial and radial kurtosis, have been reported [13, 19, 34, 41]. Such directional DK analysis may provide more precise microstructural information about the brain tissue [13, 19]. However, mean DK, directionally averaged kurtosis, has been shown to be useful in some reports, for example, investigation of glioma [38] and acute cerebral infarction

[42], among others [12, 36, 39, 40]. In MS, there has been no study using mean DK. So it is important that we report these preliminary results, because this study was able to demonstrate the clinical potential of DKI for assessing NAWM in MS patients.

Conclusion

DKI has been demonstrated to be a sensitive quantitative indicator in addition to conventional diffusional evaluations, for example DTI. DKI can provide new information about NAWM changes in MS by detecting subtle changes in brain tissue microstructure.

Acknowledgments This study was partly supported by a Grant-in-Aid for Scientific Research on Innovative Areas (Comprehensive Brain Science Network) from the Ministry of Education, Science, Sports and Culture of Japan.

References

1. Le Bihan D, Mangin JF, Poupon C, Clark CA, Pappata S, Molko N, et al. Diffusion tensor imaging: concepts and applications. J Magn Reson Imaging. 2001;13:534–46.
2. Rocca MA, Cercignani M, Iannucci G, Comi G, Filippi M. Weekly diffusion-weighted imaging of normal-appearing white matter in MS. Neurology. 2000;55:882–4.
3. Cercignani M, Iannucci G, Filippi M. Diffusion-weighted imaging in multiple sclerosis. Ital J Neurol Sci. 1999;20:S246–9.
4. Horsfield MA, Lai M, Webb SL, Barker GJ, Tofts PS, Turner R, et al. Apparent diffusion coefficients in benign and secondary progressive multiple sclerosis by nuclear magnetic resonance. Magn Reson Med. 1996;36:393–400.
5. Basser PJ. Inferring microstructural features and the physiological state of tissues from diffusion-weighted images. NMR Biomed. 1995;8:333–44.
6. Guo AC, MacFall JR, Provenzale JM. Multiple sclerosis: diffusion tensor MR imaging for evaluation of normal-appearing white matter. Radiology. 2002;222:729–36.
7. Filippi M, Agosta F. Imaging biomarkers in multiple sclerosis. J Magn Reson Imaging. 2010;31:770–88.
8. Rovaris M, Agosta F, Pagani E, Filippi M. Diffusion tensor MR imaging. Neuroimaging Clin N Am. 2009;19:37–43.
9. Werring DJ, Brassat D, Droogan AG, Clark CA, Symms MR, Barker GJ, et al. The pathogenesis of lesions and normal-appearing white matter changes in multiple sclerosis: a serial diffusion MRI study. Brain. 2000;123(Pt 8):1667–76.
10. Castriota Scanderbeg A, Tomaiuolo F, Sabatini U, Nocentini U, Grasso MG, Caltagirone C. Demyelinating plaques in relapsing-remitting and secondary-progressive multiple sclerosis: assessment with diffusion MR imaging. AJNR Am J Neuroradiol. 2000;21:862–8.
11. Tsuchiya K, Hachiya J, Maehara T. Diffusion-weighted MR imaging in multiple sclerosis: comparison with contrast-enhanced study. Eur J Radiol. 1999;31:165–9.
12. Jensen JH, Helpern JA, Ramani A, Lu H, Kaczynski K. Diffusional kurtosis imaging: the quantification of non-gaussian water diffusion by means of magnetic resonance imaging. Magn Reson Med. 2005;53:1432–40.
13. Lu H, Jensen JH, Ramani A, Helpern JA. Three-dimensional characterization of non-gaussian water diffusion in humans using diffusion kurtosis imaging. NMR Biomed. 2006;19:236–47.
14. Hori M, Fukunaga I, Masutani Y, Taoka T, Kamagata K, Suzuki Y, et al. Visualizing non-Gaussian diffusion: clinical application of q-space imaging and diffusional kurtosis imaging of the brain and spine. Magn Reson Med Sci. 2012;11(4):221–8.
15. McDonald WI, Compston A, Edan G, Goodkin D, Hartung HP, Lublin FD, et al. Recommended diagnostic criteria for multiple sclerosis: guidelines from the International Panel on the diagnosis of multiple sclerosis. Ann Neurol. 2001;50:121–7.
16. Polman CH, Reingold SC, Banwell B, Clanet M, Cohen JA, Filippi M, et al. Diagnostic criteria for multiple sclerosis: 2010 revisions to the McDonald criteria. Ann Neurol. 2011;69:292–302.
17. Polman CH, Reingold SC, Edan G, Filippi M, Hartung HP, Kappos L, et al. Diagnostic criteria for multiple sclerosis: 2005 revisions to the "McDonald Criteria". Ann Neurol. 2005;58:840–6.
18. Kurtzke JF. A new scale for evaluating disability in multiple sclerosis. Neurology. 1955;5:580–3.
19. Jensen JH, Helpern JA. MRI quantification of non-Gaussian water diffusion by kurtosis analysis. NMR Biomed. 2010;23:698–710.
20. Stejeskal EO, Tanner JE. Spin diffusion measurements: spin echoes in the presence of a time-dependent field gradient. J Chem Phys. 1965;42:288–92.
21. McFarlin DE, McFarland HF. Multiple sclerosis (first of two parts). N Engl J Med. 1982;307:1183–8.
22. McFarlin DE, McFarland HF. Multiple sclerosis (second of two parts). N Engl J Med. 1982;307:1246–51.
23. Rodriguez M, Siva A, Ward J, Stolp-Smith K, O'Brien P, Kurland L. Impairment, disability, and handicap in multiple sclerosis: a population-based study in Olmsted County Minnesota. Neurology. 1994;44:28–33.
24. Vigeveno RM, Wiebenga OT, Wattjes MP, Geurts JJ, Barkhof F. Shifting imaging targets in multiple sclerosis: from inflammation to neurodegeneration. J Magn Reson Imaging. 2012;36:1–19.
25. Geurts JJ, Stys PK, Minagar A, Amor S, Zivadinov R. Gray matter pathology in (chronic) MS: modern views on an early observation. J Neurol Sci. 2009;282:12–20.
26. Fazekas F, Barkhof F, Filippi M, Grossman RI, Li DK, McDonald WI, et al. The contribution of magnetic resonance imaging to the diagnosis of multiple sclerosis. Neurology. 1999;53:448–56.
27. Barkhof F, van Walderveen M. Characterization of tissue damage in multiple sclerosis by nuclear magnetic resonance. Philos Trans R Soc Lond B Biol Sci. 1999;354:1675–86.
28. Miki Y, Grossman RI, Udupa JK, van Buchem MA, Wei L, Phillips MD, et al. Differences between relapsing-remitting and chronic progressive multiple sclerosis as determined with quantitative MR imaging. Radiology. 1999;210:769–74.
29. Miki Y, Grossman RI, Udupa JK, Wei L, Polansky M, Mannon LJ, et al. Relapsing-remitting multiple sclerosis: longitudinal analysis of MR images—lack of correlation between changes in T2 lesion volume and clinical findings. Radiology. 1999;213:395–9.
30. Phillips MD, Grossman RI, Miki Y, Wei L, Kolson DL, van Buchem MA, et al. Comparison of T2 lesion volume and magnetization transfer ratio histogram analysis and of atrophy and measures of lesion burden in patients with multiple sclerosis. AJNR Am J Neuroradiol. 1998;19:1055–60.
31. Werring DJ, Clark CA, Barker GJ, Thompson AJ, Miller DH. Diffusion tensor imaging of lesions and normal-appearing white matter in multiple sclerosis. Neurology. 1999;52:1626–32.
32. Bammer R, Augustin M, Strasser-Fuchs S, Seifert T, Kapeller P, Stollberger R, et al. Magnetic resonance diffusion tensor imaging

for characterizing diffuse and focal white matter abnormalities in multiple sclerosis. Magn Reson Med. 2000;44:583–91.
33. Abdallah CG, Tang CY, Mathew SJ, Martinez J, Hof PR, Perera TD, et al. Diffusion tensor imaging in studying white matter complexity: a gap junction hypothesis. Neurosci Lett. 2010;475: 161–4.
34. Lazar M, Jensen JH, Xuan L, Helpern JA. Estimation of the orientation distribution function from diffusional kurtosis imaging. Magn Reson Med. 2008;60:774–81.
35. Iraji A, Davoodi-Bojd E, Soltanian-Zadeh H, Hossein-Zadeh GA, Jiang Q. Diffusion kurtosis imaging discriminates patients with white matter lesions from healthy subjects. In: Proceedings of the 33rd international conference of the IEEE engineering in medicine and biology society. 2011. p. 2796–9.
36. Falangola MF, Jensen JH, Babb JS, Hu C, Castellanos FX, Di Martino A, et al. Age-related non-Gaussian diffusion patterns in the prefrontal brain. J Magn Reson Imaging. 2008;28:1345–50.
37. Cheung MM, Hui ES, Chan KC, Helpern JA, Qi L, Wu EX. Does diffusion kurtosis imaging lead to better neural tissue characterization? A rodent brain maturation study. Neuroimage. 2009;45: 386–92.
38. Raab P, Hattingen E, Franz K, Zanella FE, Lanfermann H. Cerebral gliomas: diffusional kurtosis imaging analysis of microstructural differences. Radiology. 2010;254:876–81.
39. Grossman EJ, Ge Y, Jensen JH, Babb JS, Miles L, Reaume J, et al. Thalamus and cognitive impairment in mild traumatic brain injury: a diffusional kurtosis imaging study. J Neurotrauma. 2012;29:2318–27.
40. Zhuo J, Xu S, Proctor JL, Mullins RJ, Simon JZ, Fiskum G, et al. Diffusion kurtosis as an in vivo imaging marker for reactive astrogliosis in traumatic brain injury. Neuroimage. 2012;59: 467–77.
41. Helpern JA, Adisetiyo V, Falangola MF, Hu C, Di Martino A, Williams K, et al. Preliminary evidence of altered gray and white matter microstructural development in the frontal lobe of adolescents with attention-deficit hyperactivity disorder: a diffusional kurtosis imaging study. J Magn Reson Imaging. 2011;33:17–23.
42. Hori M, Aoki S, Fukunaga I, Suzuki Y, Masutani Y. A new diffusion metric, diffusion kurtosis imaging, used in the serial examination of a patient with stroke. Acta Radiol Sh Rep. 2012;1:2.
43. Trampel R, Jensen JH, Lee RF, Kamenetskiy I, McGuinness G, Johnson G. Diffusional kurtosis imaging in the lung using hyperpolarized 3He. Magn Reson Med. 2006;56:733–7.
44. Allen IV, McQuaid S, Mirakhur M, Nevin G. Pathological abnormalities in the normal-appearing white matter in multiple sclerosis. Neurol Sci. 2001;22:141–4.